In spite of the inescapable tangle between the metal-metal and the metal-ligand-metal contributions to the stability of bridged dimers, the existence of very long bonds in some Zr(III) dimers had been suggested recently by several experimental[5-7] and theoretical[7,8] investigations. The present ab initio calculations provide evidence that the bond lengths observed in $[Cp_2Zr(\mu\text{-}X)]_2$ dimers and the reported diamagnetism of those molecules can be explained only by such "superlong" metal-metal σ bonds. The abnormally large Zr-Zr bond lengths are explained by the existence of steric repulsions that develop between the cyclopentadienyl ligands in the cis position with respect to the dimetal unit. This repulsion had been estimated previously by means of SCF calculations to reach 6 kcal·mol^{-1} for $[(C_5H_5)_2Zr(\mu\text{-}PH_2)]_2$ at the observed geometry ($d_{Zr\text{-}Zr}$ = 3.65 Å).[8] Since the Zr-Zr σ bond is expected to act as a restoring force balancing the steric repulsion, this value of 6 kcal·mol^{-1} could therefore fix an order of magnitude to the stabilization energy attributable to the "superlong" Zr-Zr bond. The comparable structures[7,36] and the diamagnetism of Hf(III) dinuclear complexes[36] suggest that a similar rationalization should hold for those dimers. In contrast to that, the 3d orbitals of titanium, more contracted and less polarizable, cannot overlap enough to balance the steric repulsion of the opposite Cp rings. The metal-metal distances then become larger than 3.7 Å, and the Ti-Ti interaction is reduced to an antiferromagnetic coupling.

(36) (a) Cotton, F. A.; Kibala, P. A.; Wojtczak, W. A. *Inorg. Chim. Acta* **1990**, *177*, 1. (b) Girolami, G. S.; Wilson, S. R.; Morse, P. M. *Inorg. Chem.* **1990**, *29*, 3200.

The weakening of the metal-metal σ overlap when the metallacycle flattens finds another origin in the region of nonbonding charge concentration generated around the center of symmetry of the system by the close contact of the bridging ligand lone pairs. The presence of this charge density generates a repulsive interaction with the metal-metal bonding combination of d_{z^2} orbitals, which responds by progressively transforming into a nonbonding d_{y^2} combination. In the considered range of distances (3.0-4.0 Å) this rehybridization is slow and partial for Zr(III) dimers, which retain significant σ character up to $d_{Zr\text{-}Zr}$ = 4 Å. Conversely, the transformation into d_{y^2} orbitals is already complete for bridged Ti(III) dimers at $d_{Ti\text{-}Ti}$ = 3.65 Å.

As for the $[Cp_2Ti(\mu\text{-}X)]_2$ complexes, the electronic structure of $[Cp(\mu\text{-}\eta^1\text{:}\eta^5\text{-}C_5H_4)Ti(PMe_3)]_2$, belonging to the C_2 point group, can be rationalized in terms of coupled Cp_2ML_3 fragments. At variance from the C_{2v} complexes, however, no steric repulsion develops between the Cp cycles, and the metal-metal σ coupling occurs through the overlap of *lateral* hybrid orbitals of the Cp_2Ti fragments. A relatively short metal-metal distance (3.223 Å) can therefore be observed, and the Ti-Ti σ overlap is not hindered by charge concentrations arising from the other ligands. A rather strong Ti-Ti σ bond is then obtained in spite of the slight tilt angle (21°) of the overlapping metal orbitals.

Acknowledgment. All calculations have been carried out on the CRAY-2 computer of the CCVR (Palaiseau, France) through a grant of computer time from the Conseil Scientifique du Centre de Calcul Vectoriel pour la Recherche.

Geometry Optimization through Second-Moment Scaling

L. M. Hoistad, S. Lee,* and J. Pasternak

Contribution from the Department of Chemistry, University of Michigan, 930 North University Avenue, Ann Arbor, Michigan 48109-1055. *Received November 22, 1991*

Abstract: We show that second-moment-scaled Hückel theory can be used to account for the bond length variations found in elemental gallium, borohydride, transition metal carbonyl, and hydrocarbon structures. Among the systems investigated are Ga, $B_8H_8^{2-}$, $B_9H_9^{2-}$, $B_{10}H_{10}^{2-}$, $Os_5(CO)_{16}$, $Ir_4(CO)_{12}$, $[Re_4(CO)_{16}]^{2-}$, buckminsterfullerene, naphthalene, spiropentane, and butadiene. We also show that the second-moment-scaled Hückel theory correctly resolves the differences in energies among the closo, nido, and arachno borohydride cluster forms. These latter results are in good agreement with Wade's rules for clusters. Finally, we discuss the underlying assumptions of second-moment-scaled theory.

Much of our understanding of the variations in bond distances comes from extended Hückel (eH) molecular orbital calculations and overlap population analyses. This latter technique has been successfully applied to the full range of chemical compounds including main group, transition metal, molecular, and solid-state systems. The overlap population method and its applications have been well reviewed.[1] Briefly, in this method one holds all bonds of a given type (e.g., C-C or B-B bonds) at the same single length. One then calculates the net amount of in-phase or out-of-phase atomic overlap in all the occupied molecular orbitals for a specific pair of atoms. This net amount of overlap is the overlap population.[2] It is found that this overlap population correlates well with the actual bond distances.

This technique however has a shortcoming in that one cannot in general deduce quantitatively the variations in bond lengths.[3] In part, the reason for this is the difficulty one has of studying directly changes in bond lengths with Hückel molecular orbital calculations. Indeed, it is for this reason that one holds bond length constant in deriving useful overlap populations.

Recently, a new modification of Hückel molecular orbital theory has been introduced which obviates the need for careful adjustment of bond lengths.[4] This modification, which we call second-moment scaling, has been proven successful in rationalizing crystalline structure type as a function of electron count for a variety of

* Author to whom correspondence should be addressed.

(1) Discussions of the overlap population method are given in: (a) Albright, T. A.; Burdett, J. K.; Whangbo, M.-H. *Orbital Interactions in Chemistry*; Wiley: New York, 1985; p 21. (b) Salem, L. *The Molecular Orbital Theory of Conjugated Systems*; Benjamin: New York, 1966; p 134.

(2) The formal definition for overlap population between two atomic orbitals Φ_μ and Φ_ν is $P_{\mu\nu} = \sum_i 2N_i C_{\mu i} C_{\nu i} S_{\mu\nu}$, where N_i is the occupation of the ith molecular orbital, $S_{\mu\nu}$ is the overlap integral between Φ_μ and Φ_ν, and $C_{\mu i}$ and $C_{\nu i}$ are the LCAO coefficients for the ith molecular orbital.

(3) It should be noted that in the case of unsaturated hydrocarbons one can find a quantitative relation between overlap population and bond lengths. See: Coulson, C. A.; Golebiewski. *Proc. Phys. Soc., London* **1961**, *78*, 1310.

(4) Early applications of the second moment scaling hypothesis are given in: (a) Pettifor, D. G.; Podloucky, R. *Phys. Rev. Lett.* **1984**, *53*, 1080. (b) Burdett, J. K.; Lee, S. *J. Am. Chem. Soc.* **1985**, *107*, 3063. More recent work: (c) Cressoni, J. C.; Pettifor, D. G. *J. Phys.: Condens. Matter*, submitted for publication. (d) Lee, S. *J. Am. Chem. Soc.* **1991**, *113*, 101. (e) Lee, S. *J. Am. Chem. Soc.* **1991**, *113*, 8216. (f) Hoistad, L. M.; Lee, S. *J. Am. Chem. Soc.* **1991**, *113*, 8216. (g) Lee, S. *Acc. Chem. Res.* **1991**, *24*, 249.

0002-7863/92/1514-4790$03.00/0

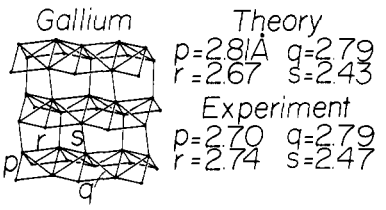

Figure 1. Crystal structure of elemental gallium. Using the *Abma* space group convention, the *b* axis is in the horizontal direction, the *c* axis is in the vertical direction, and the *a* axis is perpendicular to the plane of the paper. There are four inequivalent bond lengths in this structure which we label *p*, *q*, *r*, and *s*. Experimental values are from single-crystal X-ray studies, while theoretical values are from our second-moment-scaled calculations. Hückel parameters used in this calculation are shown in Table I. We used an orthorhombic 27-k-point mesh in our optimization.

Table I. Hückel Atomic Parameters

atom	orbital	H_{ii}, eV	ζ_1	ref
B	2s	−15.2	1.30	5b
	2p	−8.5	1.30	
C	2s	−21.4	1.625	5a
	2p	−11.4	1.625	
H	1s	−13.6	1.30	5a
Ir, Os, Re	6s	−9.36	2.398	5j
	6p	−5.96	2.372	
	5d[a]	−12.66	5.343 (0.6662)	
Ga, Ge	4s	−16.0	2.16	5k
	4p	−9.0	1.85	

[a] ζ_2 = 2.277 (0.5910).

systems ranging from intermetallic compounds and alloys to transition and main group elemental structures. In this model one assumes the repulsive interaction between atoms can be accounted for indirectly by changing the bandwidth of a Hückel or extended Hückel calculation. In particular, one fixes the overall variance of the Hückel molecular orbitals to a set value. The variance is defined to be

$$\frac{1}{n}\sum_{i=1}^{n}(E_i - E_{\text{avg}})^2$$

where E_i's are the molecular orbital energies, E_{avg} is the average orbital energy, and there are a total of n molecular orbitals in the system. We discuss the underlying assumptions of this method in the Appendix.

In applying this method, we adopt the following general procedure. We first calculate the total Hückel electronic energy of each of the crystal structure types that we wish to study. These total energies are then scaled so as to have the same overall variance. It is usually convenient to select one structure and to then scale all variances to the value originally calculated for this selected compound. In practice, we change the overall density of the structures in an iterative process until the variance equals that of the selected compound. Other than this, we use a standard Hückel method in our band calculations. The diagonal matrix elements of our Hückel Hamiltonian are taken from a set of parameters developed by Hoffmann and others.[5] We use the Wolfsberg–Helmholz approximation in calculating off-diagonal matrix elements.[6] Unlike the manner in which extended Hückel

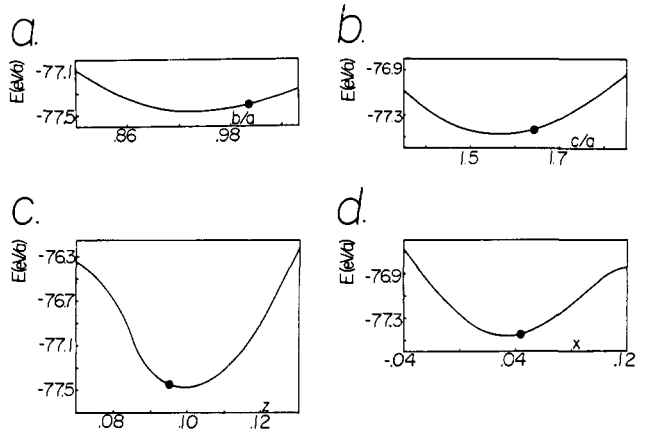

Figure 2. Total energy per atom in elemental gallium as a function of the *b*/*a*, *c*/*a*, *z*, and *x* structural parameters. The dark circles indicate the known experimental values for these parameters. Hückel parameters used in this calculation are shown in Table I.

calculations are performed, we solve the secular equation $H\Psi = E\Psi$ and not $H\Psi = ES\Psi$.

This method has been used primarily as a tool for making structure maps as a function of electron count.[4,7] For example, we find for alloys that the γ-brass structure is the most stable structure type near 11.65 s, p, and d valence electrons per atom (e/a), while the hexagonal closest-packed structure is stable between 11.75 and 12.00 s, p, and d e/a.[4f,8] However, as of yet, we have not used this method to resolve the variation in bond lengths of a given structure type. Let us consider for example elemental gallium. We have recently shown that the elemental gallium structure, illustrated in Figure 1, is of lower energy than other main group structures such as the diamond or the face-centered-cubic structure near 3 s and p e/a. However, elemental gallium has orthorhombic crystal symmetry. Hence it has three variable cell parameters which correspond to the *a*, *b*, and *c* axis lengths. Furthermore, the elemental gallium structure type also contains two atomic parameters *x* and *z* which control the position of the gallium atoms within the unit cell.[10] These cell and atomic parameters determine the bond distances and the bond angles within the gallium crystal. As the goal of our current work is to calculate reliably the variations of bond distances, we need to devise a technique which predicts the values of these positional parameters. In this paper, we will adopt the following general procedure to determine positional parameters. In all cases, we begin with a trial solution for the values of the positional parameters. We then vary a single positional parameter while holding all other parameters constant so as to determine the value of this chosen parameter which minimizes the total Hückel energy. We proceed in an iterative fashion until a fully convergent solution is reached. By way of verification that this minimum-energy solution is indeed the global minimum, we consider alternate initial trial solutions.

(5) Many important atomic parameters are reported in the following: (a) Hoffmann, R. *J. Chem. Phys.* **1963**, *39*, 1397. (b) Hoffmann, R.; Anderson, A. B. *J. Chem. Phys.* **1974**, *60*, 4271. (c) Hoffmann, R.; Rossi, A. R. *Inorg. Chem.* **1975**, *14*, 365. (d) Hay, P. J.; Thibeault, J. C.; Hoffmann, R. *J. Am. Chem. Soc.* **1975**, *97*, 4884. (e) Hoffmann, R.; Elian, M. *Inorg. Chem.* **1975**, *14*, 1058. (f) Hoffmann, R.; Summerville, R. H. *J. Am. Chem. Soc.* **1976**, *98*, 7240. (g) Komiya, S.; Albright, T. A.; Hoffmann, R. *Inorg. Chem.* **1978**, *17*, 126. (h) Hughbanks, T.; Hoffmann, R.; Whangbo, M.-H.; Stewart, K. R.; Eisenstein, O.; Canadell, E. *J. Am. Chem. Soc.* **1982**, *104*, 3876. (i) Chen, M. M. L.; Hoffmann, R. *J. Am. Chem. Soc.* **1976**, *98*, 1647. (j) Dedieu, A.; Albright, T. A.; Hoffmann, R. *J. Am. Chem. Soc.* **1979**, *101*, 3141. (k) Thorn, D. L.; Hoffmann, R. *Inorg. Chem.* **1978**, *17*, 126.

(6) Wolfsberg, M.; Helmholz, L. *J. Chem. Phys.* **1957**, *20*, 83.

(7) (a) Zunger, A. *Phys. Rev. B* **1980**, *22*, 5839. (b) Burdett, J. K.; Price, G. D.; Price, S. L. *Phys. Rev. B* **1981**, *24*, 2903. (c) Pettifor, D. G. *Solid State Commun.* **1984**, *51*, 37. (d) Pettifor, D. G. *J. Phys. C* **1986**, *19*, 285.

(8) Both the γ-brass and hexagonal closest-packed structures are electron compounds. The term "electron compounds" denotes a structure type whose range of stability is determined by the number of valence electrons per atom. It is well established that the electron counts listed in the text for these two materials which are the result of our earlier calculations (see ref 4f) are in fact in close agreement with the true experimental values. See discussion in: Hume-Rothery, W.; Raynor, G. V. *The Structure of Metals and Alloys*; Institute of Metals: London, 1962; p 194.

(9) A preliminary communication on the $B_8H_8^{2-}$, $B_9H_9^{2-}$, and $B_{10}H_{10}^{2-}$ calculations is reported in: Hoistad, L. M.; Lee, S.; Chou, D. C. *R. Acad. Sci., Ser. 2* **1991**, *313*, 159.

(10) We have used the following nonstandard space group in our calculations. First, we follow much of the literature and adopt the *Abma* setting for the orthorhombic axes. Second, we place the gallium atoms at the eight symmetry-equivalent sites $(x, 0, z)$, $(^1/_4 - x, 0, ^1/_2 - z)$, $(^1/_2 + x, 0, -z)$, $(^3/_4 - x, 0, ^1/_2 + z)$, $(x, ^1/_2, ^1/_2 + z)$, $(^1/_4 - x, ^1/_2, -z)$, $(^1/_2 + x, ^1/_2, ^1/_2 - z)$, and $(^3/_4 - x, ^1/_2, z)$. These nonstandard settings have the advantage that for values $x = 0$, $z = 0$, and $b/a = \sqrt{3}/2$ one has perfect two-dimensional closest-packed layers perpendicular to the *c* axis.

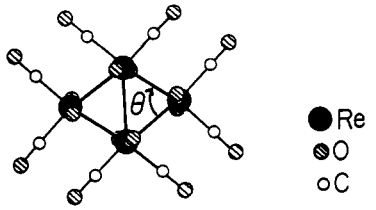

Figure 3. Structure of $[Re_4(CO)_{16}]^{2-}$.

However, in general the energy curves are relatively smooth, and hence this last step, which is necessary in the case of false minima, has not proven to be a significant issue.

For example, we have applied this method to the gallium system described above. We find the optimal values of the ratios of the cell parameters c/a and b/a are 1.61 and 0.94 as compared to experimental values of 1.69 and 0.99. Similarly, the theoretical optimal values of x and z are 0.035 and 0.100 as compared to experimental values of 0.044 and 0.095. It may be seen that the agreement between theory and experiment is good. In Figure 2 we plot the total Hückel energy as a function of these four parameters near this minimum-energy solution. In this figure it may be noted that the agreement between experiment and theory is best in the case of the steeper parabolas (e.g., the z parameter curve) and worse in the case of shallow parabolas (e.g., the b/a parameter curve). Unfortunately, it is not immediately clear how one might further interpret our displayed results. The reasons for this are 2-fold. First, we are only able to determine the values of the structural parameters a, b, c, x, and z subject to the constraint that the variance is equal to a fixed value. As variance is proportional to overlap of atomic orbitals and as overlap is in turn proportional to atomic density, we have constrained the overall molecular size. It is for this reason that in Figure 2 we have calculated only unitless quantities such as c/a, b/a, x, and z. Second, although we know such unitless parameters control the overall shape of the crystalline system, it is quite difficult in practice to convert such abstract numbers into clear geometric factors.

In order to evaluate the accuracy of our estimates of the variation in bond lengths, we have decided to present our data in a somewhat artificial but geometrically clear manner. We use the variance of the experimentally known chemical system to set the overall size of the crystal. In this manner we scale the crystal systems so that the average bond length of our theoretically optimized geometry is set roughly equal to the experimentally known average bond length. We show a list of such bond lengths for the elemental gallium structure in Figure 1. It may be seen that our calculations correctly find that one of the gallium bonds is much shorter than the other bonds (by approximately 0.3 Å). Our overall bond lengths are in general within 0.1 Å of the true distances. This error is clearly smaller than the variation in bond distances, and therefore our results are statistically significant.

It is important to note that while the overall size factor derived from second-moment scaling is important in determining the average bond length, it has little effect on unitless quantities such as the ratio of bond distances. As a simple demonstration, we consider the $[Re_4(CO)_{16}]^{2-}$ ion.[11] This ion is illustrated in Figure 3. It may be seen in this figure that one of the structural parameters is the unitless parameter θ, the bond angle which controls the length of the transannular Re–Re bond. In experimentally observed $[Re_4(CO)_{16}]^{2-}$, the θ angle is 59.04°. We have calculated the optimal value for this θ angle for three different Re–Re average bond lengths. We chose average bond distances of 2.99, 2.69, and 3.29 Å. The first value corresponds to the true experimental average, while for the last two we have changed this average by ±10%. These last two bond distances represent extreme values; average Re–Re bond lengths shorter than 2.69 Å or longer than 3.29 Å are not chemically reasonable. Nevertheless, for each of these three cases, we find the optimal value for the unitless θ parameter is essentially constant. For the 2.69, 2.99, and 3.29 Å average bond distance, we find respectively θ values of 60.7, 59.9, and 58.5°. This is a clear illustration that our method can indeed estimate unitless structural parameters without recourse to exact second-moment values derived from experimental geometries.

(11) Churchill, M. R.; Bau, R. *Inorg. Chem.* **1968**, *7*, 2606.

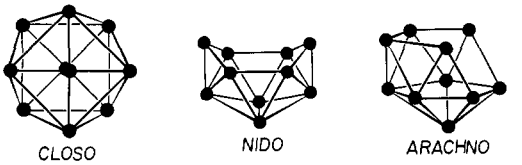

Figure 4. Closo, nido, and arachno geometries. We show here the location of the boron atoms in respectively $B_{10}H_{10}^{2-}$, $B_{10}H_{10}^{4-}$, and $B_{10}H_{10}^{6-}$.

Borohydrides

The same method may be applied to molecular systems as well. As our first series of examples, we will consider the borohydrides, which are a large family of electron-deficient clusters.[12] A few of these clusters are illustrated in Figure 4. Borohydrides have been well studied by theorists. It is well accepted today that their structures can be understood through the use of Wade's rules and molecular orbital theory.[13] However, to our knowledge the calculations we present in this article are the first calculations of the Hückel type predicting the variation in bond lengths in these cluster systems.

Borohydride clusters are generally divided into the closo, the nido, and the arachno deltahedral families. An example of each of these three families is shown in Figure 4. It may be seen that the closo forms are the most symmetric clusters. They are the parent clusters from which the nido and arachno clusters can be derived. We therefore have begun our study of borohydride clusters with the closo family of structures. These include the set of ions $B_nH_n^{2-}$ where $n = 6$–12. Among this set, the ions $B_7H_7^{2-}$ and $B_{11}H_{11}^{2-}$ have never been resolved by single-crystal X-ray studies. In the absence of good structural data, $B_7H_7^{2-}$ and $B_{11}H_{11}^{2-}$ are not good test cases as to the reliability of our calculational method. Similarly, $B_6H_6^{2-}$ and $B_{12}H_{12}^{2-}$ are also not useful systems for study. This is because these latter two clusters have respectively octahedral and icosahedral point symmetries and therefore have only one type of B–B bond length. Hence they are not suitable for a direct study of bond length variation. We therefore consider here the three remaining closo structures, $B_8H_8^{2-}$, $B_9H_9^{2-}$, and $B_{10}H_{10}^{2-}$.[14]

We consider first the $B_{10}H_{10}^{2-}$ cluster, which has D_{4d} point group symmetry (see Figure 4). There are a total of 24 positional B parameters in this system if one allows all possible distorting motions. With our rather straightforward technique of finding the minimum-energy surface, it is difficult for us to find the minimum for this number of variables. We have therefore chosen to limit the number of positional parameters. This is analogous to the procedure we adopted in the preceding section for elemental gallium. In this earlier analysis, we limited ourselves to five parameters by fixing the *Abma* space group symmetry. For $B_{10}H_{10}^{2-}$ there are only three positional parameters, assuming a D_{4d} point group symmetry. We therefore use the iterative procedure described in the preceding section to find the values for these parameters which minimize the total electronic energy. As before, we have optimized the overall geometry subject to the constraint that the variance is equal to that found for the true experimental geometry.

It may be noted that there is one marked difference between elemental gallium and the borohydride systems. In the former

(12) A recent overview is given in: Olah, G. A.; Wade, K.; Williams, R. E. *Electron Deficient Boron and Carbon Clusters*; Wiley: New York, 1991.

(13) (a) Wade, K. *Adv. Inorg. Chem. Radiochem.* **1976**, *18*, 1. (b) Rudolph, R. W.; Pretzer, W. R. *Inorg. Chem.* **1972**, *11*, 1974. (c) Williams, R. E. *Inorg. Chem.* **1971**, *10*, 210. (d) Stone, A. J. *Inorg. Chem.* **1981**, *20*, 563. (e) Mingos, D. M. P. *Acc. Chem. Res.* **1984**, *17*, 311.

(14) (a) $B_8H_8^{2-}$: Guggenberger, L. J. *Inorg. Chem.* **1969**, *8*, 2771. (b) $B_9H_9^{2-}$: Guggenberger, L. J. *Inorg. Chem.* **1968**, *7*, 2261. (c) $B_{10}H_{10}^{2-}$: Gill, J. T.; Lippard, S. J. *Inorg. Chem.* **1975**, *14*, 751.

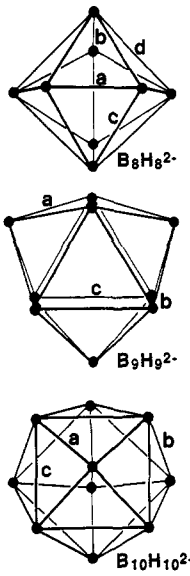

	Experiment	Theory
a=	1.56Å	1.54Å
b=	1.72	1.64
c=	1.76	1.82
d=	1.93	1.90
a=	1.71Å	1.70Å
b=	1.84	1.75
c=	1.90	1.98
a=	1.68Å	1.65Å
b=	1.79	1.79
c=	1.82	1.87

Figure 5. Experimental and theoretically derived bond lengths for $B_8H_8^{2-}$, $B_9H_9^{2-}$, and $B_{10}H_{10}^{2-}$. For experimental values we have averaged the bond lengths which should be equivalent in respectively ideal D_{2d}, D_{2h}, and D_{4d} point group symmetries. Hückel parameters used in this calculation are shown in Table I.

all bonds are homoatomic, while in the latter system there are B–H bonds in addition to B–B bonds. This is important, as the second-moment scaling technique can be applied only to purely covalent bonds, where there is little or no charge transfer. However, changing the boron–hydrogen bond distance would result in exactly this sort of unwanted charge transfer. We therefore consider only variations of the B–B bonds and fix the B–H bonds to a constant and reasonable length. Furthermore, we require that the B–H bonds point in a purely radial manner with respect to the center of the cluster. In Figure 5 we compare the theoretically determined minimum-energy geometry to the true experimental structure. It may be seen that there is good agreement between theory and experiment.

The same holds for other borohydrides such as $B_8H_8^{2-}$ and $B_9H_9^{2-}$ as well. We show in Figure 5 a comparison of observed and calculated bond distances for these clusters where we have assumed $B_8H_8^{2-}$ and $B_9H_9^{2-}$ have respectively D_{2d} and D_{3h} symmetries. For all the species shown in Figure 5, we find the theoretical calculations determine which bonds should be longest and which should be weakest in any given structure. Furthermore, all calculated distances are within 0.10 Å of the true bond distances and in most cases the error is less than 0.05 Å.

Transition Metal Carbonyl Clusters

Another well-known family of cluster compounds is transition metal carbonyl compounds. It is generally accepted today that these compounds follow the same electron-counting rules as the borohydrides discussed in the previous section.[13a] In this scheme, the boron atoms and hydrogen atoms are replaced by respectively transition metal atoms and carbonyl (carbon monoxide) groups. There are however several important structural differences between transition metal carbonyl clusters and the borohydride ones. First, the resemblance of transition metal clusters to the borohydride compounds is clear only in small clusters which contain six or fewer metal atoms. Second, the large majority of transition metal carbonyl compounds contain bridging carbonyl ligands, i.e., carbonyl groups which are simultaneously bonded to more than one transition metal atom. This is in sharp contrast to the closo borohydrides, which have only nonbridging (terminal) hydrogen atoms. Third, the ratio of carbonyl groups per transition metal atom is much higher than the corresponding ratio between hydrogen and boron atoms.

These structural differences have a direct consequence as to the systems that we can study with our second-moment scaling method. Due to the first difference enumerated above, we will

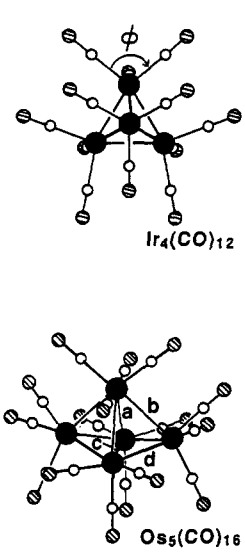

	Experiment	Theory
ϕ=	96.60	96.68
a=	2.87Å	3.01Å
b=	2.89	2.94
c=	2.75	2.71
d=	2.75	2.65

Figure 6. Structures of $Ir_4(CO)_{12}$ and $Os_5(CO)_{16}$.

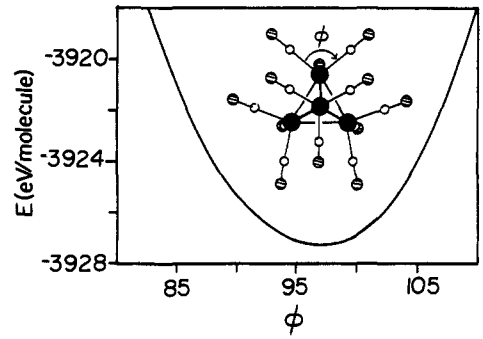

Figure 7. Energy of $Ir_4(CO)_{12}$ as a function of the C–Ir–C bond angle, ϕ. See Table I for a listing of the Hückel parameters used in this calculation.

study only smaller transition metal clusters, as we wish to study compounds which are analogous to our borohydride systems. Secondly, we will consider only the comparatively few transition metal systems which do not contain bridging carbonyl ligands. The reason for this second restriction may be understood if we recall that we can only study homoatomic bond breakage; cleavage of metal atoms bridged by a single carbonyl group would perforce break a heteroatomic metal–carbon bond.

Finally, the last structural difference discussed above, i.e., the high ratio of carbonyl groups to metal atoms, results in new structural parameters. These correspond to bond angles between metal atoms and carbonyl groups. They must now also be considered. As a simple example of this last difference, we turn to the $Ir_4(CO)_{12}$ molecule.[15] This molecule has tetrahedral (T_d) symmetry and is illustrated in Figure 6. If we require the molecule to be of T_d symmetry, there are only four variable parameters. These are the Ir–Ir, Ir–C, and C–O bond lengths and the C–Ir–C bond angle, ϕ. In our method of geometry optimization, we hold all ligand bond lengths constant. We therefore set the Ir–C and C–O bond lengths at reasonable and fixed values. Furthermore, the overall fixed second moment eliminates the Ir–Ir bond as a structural variable. Hence the only remaining variable is ϕ. In Figure 7 we show the energy dependence of the molecule as a function of ϕ, where we have scaled the variance to the experimentally determined value. The function is essentially a parabola with a minimum energy at $\phi = 96.68°$. This compares to the experimentally known value of 96.60°. It may be seen that our calculated value falls within the experimental error of the known geometry. Agreement between theory and experiment is essentially perfect.

(15) Churchill, M. R.; Hutchinson, J. P. *Inorg. Chem.* **1978**, *17*, 3528.

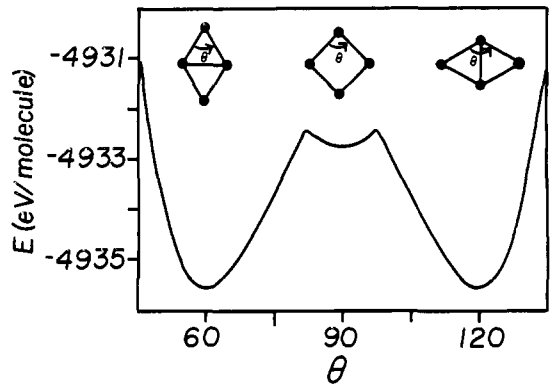

Figure 8. Energy of $[Re_4(CO)_{16}]^{2-}$ as a function of the Re–Re–Re bond angle, θ. See Table I for the Hückel parameters used in this calculation.

We can consider other more complicated geometries. We have examined the geometry of $[Re_4(CO)_{16}]^{2-}$, which has the D_2 symmetry illustrated in Figure 3. As our principal interest is the energetics of metal–metal bonds, we fix the individual carbonyl groups at fixed angles. In this manner we turn each $Re(CO)_4$ unit into a rigid body whose orientation is fixed relative to the center of the cluster. As the overall variance is set by the experimental geometry, only one structural parameter remains. This is the angle θ shown in Figure 3. We show in Figure 8 the total energy of this species as a function of θ. It may be seen that this function is symmetrical around the value of $\theta = 90°$. This symmetry corresponds to the square geometry found when $\theta = 90°$. The theoretically calculated minima for θ are 59.95 and 120.05°. This agrees closely with the experimental value of $\theta = 59.04°$. Figure 8 also shows that $[Re_4(CO)_{16}]^{2-}$ is not a fluxional species; indeed, the barrier height between the two stable geometries is over 3 eV/molecule.

As a last example, we consider the $Os_5(CO)_{16}$ molecule, which is also illustrated in Figure 6.[16] In this molecule, four of the five Os atoms have three terminal CO ligands, while the fifth Os is attached to four carbonyl groups. This slight asymmetry lowers the molecule from D_{3h} to C_{2v} symmetry. As in the preceding example, we treat the four $Os(CO)_3$ and the single $Os(CO)_4$ molecules as rigid bodies whose orientation is fixed relative to the cluster center. These constraints leave a total of three variable parameters for our optimization procedure. As may be seen in Figure 6, the agreement between experimental and theoretical bond distances is reasonable. Of the four Os–Os bond types, it is experimentally observed that two are longer, while the remaining two are shorter. Our calculations correctly reproduce this result. Finally, no calculated bond distance deviates from the true experimental distances by more than 0.1 Å.

Hydrocarbons

Hückel and eH methods were originally developed to understand structural features of hydrocarbon molecules. Using the Hückel method one can show there is a quantitative relationship between bond length and the calculated Hückel bond order. One can therefore reasonably expect that our calculational method can be used to optimize hydrocarbon geometries. However, it should be noted that as the original Hückel and eH calculations show good correlation between the overlap population of bonded atoms and their bond length, the structural consequences of overlap populations between nonbonded atoms can only be small.[3] This presents us with a clear problem. The accepted carbon Slater-type orbitals (STO) lead to strong interatomic overlaps at distances greater than those found for first-nearest neighbors.

We have therefore optimized the geometry of several hydrocarbons by our second-moment-scaling technique using two different techniques. In the first set of calculations we considered nonzero off-diagonal terms in our Hamiltonian only between bonded atoms, while in the second set we considered all overlaps in determining the Hamiltonian. In particular, we considered the molecules naphthalene, butadiene, spiropentane, and buckminsterfullerene (C_{60}). These molecules have respectively D_{2h}, C_{2h}, D_{2d}, and I_h point group symmetries. They are illustrated in Figure 9. There are four variable parameters for naphthalene, two for butadiene, one for spiropentane, and one for buckminsterfullerene. Table II illustrates the reasonable agreement found between the theoretically minimized geometries of these molecules and their true geometries.[17] It may be seen that the model where we consider only nearest-neighbor interactions produces on the whole a more reasonable estimate of bond length variations. It is interesting to note that we observed a similar effect in earlier work in comparing silicide structures such as $ThSi_2$ and $ZrSi_2$.[4,18]

Table II. Experimental and Theoretically Calculated Bond Lengths (Å) and Angles (deg) of Some Carbon-Containing Molecules[a]

naphthalene	spiropentane	butadiene	buckminsterfullerene
	Experimental		
$a = 1.418$	$a = 1.519$	$a = 1.463$	$a = 1.432$
$b = 1.421$	$b = 1.469$	$b = 1.341$	$b = 1.388$
$c = 1.364$	$\theta = 62.2$	$\theta = 123.3$	
$d = 1.415$			
	Calculated: Nearest-Neighbor Only		
$a = 1.448$	$a = 1.517$	$a = 1.597$	$a = 1.497$
$b = 1.421$	$b = 1.470$	$b = 1.288$	$b = 1.301$
$c = 1.330$	$\theta = 62.1$	$\theta = 127.3$	
$d = 1.436$			
	Calculated: All Interactions Considered[b]		
$a = 1.594$	$a = 1.496$	$a = 1.642$	
$b = 1.409$	$b = 1.495$	$b = 1.269$	
$c = 1.332$	$\theta = 60.0$	$\theta = 127.6$	
$d = 1.419$			

[a] See Figure 9 for the locations of the various bonds. [b] When all orbital interactions are considered, C_{60} is not a stable configuration.

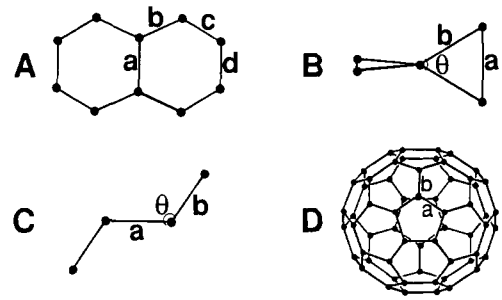

Figure 9. Structures of some carbon-containing molecules: (A) naphthalene ($C_{10}H_8$); (B) spiropentane (C_5H_8); (C) butadiene (C_4H_6); (D) buckminsterfullerene (C_{60}). Black circles indicate the locations of the carbon atoms. The letters a, b, c, d, and θ refer to inequivalent bond distances and bond angles. See Table II for calculated values.

Wade's Rules

The previous results clearly illustrate that if we know the point group symmetry of a given molecule, we are then able to calculate accurately with our method the unitless structural parameters of that molecule. It is clear that our method would be even more effective were we able to optimize geometries without knowledge

(16) Reichert, B. E.; Sheldrick, G. M. *Acta Crystallogr.* **1977**, *B33*, 173.

(17) Buckminsterfullerene: Hawkins, J. M.; Meyer, A.; Lewis, T. A.; Loren, s.; Hollander, F. J. *Science* **1991**, *252*, 312. Parameters for hydrocarbons can be found in: Dewar, M. J. S.; Theil, W. *J. Am. Chem. Soc.* **1977**, *99*, 4908.

(18) Some insight into the true energetic importance of non-nearest-neighbor interactions may be garnered from a comparison of the relative stability of carbon in the diamond and graphite structural forms. As is well-known, these two structures have nearly the same energy. In our model using only nearest-neighbor interactions we find that diamond is more stable than graphite by 0.6 eV/atom. However, when all orbital interactions are considered, graphite is lower in energy by 1.7 eV/atom. These results imply that the energetic role of second and further neighbors is nonnegligible but that our calculations overestimate their energetic importance.

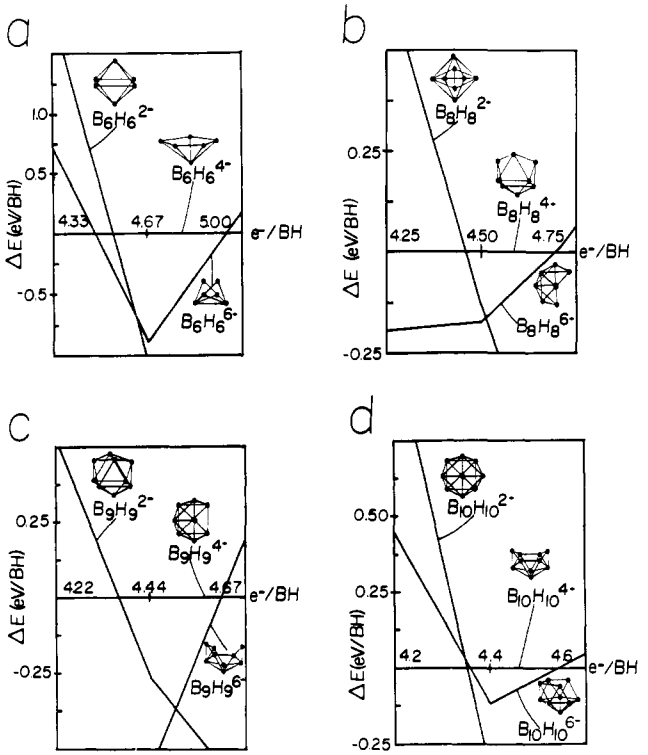

Figure 10. Differences in energy among the closo, nido, and arachno forms as a function of the number of electrons per BH formula unit for (a) 6-vertex polyhedra, (b) 8-vertex polyhedra, (c) 9-vertex polyhedra, and (d) 10-vertex polyhedra. The curves plotted are the differences in energy between the given structures and the *nido* forms. See text for further figure conventions. Note on the x axis we indicate in all graphs three different electron count values. These correspond to the electron counts of the experimentally known closo, nido, and arachno structures. Thus in (a), $B_6H_6^{2-}$, $B_6H_6^{4-}$, and $B_6H_6^{6-}$ have respectively 4.33, 4.67, and 5.00 valence electrons per BH formula unit.

of the point group symmetry. Unfortunately, the removal of this limitation leads in general to an unwieldy number of parameters. For example, in our calculation on $B_{10}H_{10}^{2-}$, we had to consider only three parameters when we restricted ourselves to D_{4d} symmetry. Removal of the symmetry constraint leads to at least 24 parameters, which is too large a number for us to treat directly.

However, we have some results on borohydride systems which indicate that this point group symmetry constraint may not be a firm requirement for our method. For borohydride systems, we have indeed compared molecules with different point group symmetries. For example, it is known that $B_{10}H_{10}^{2-}$ forms the closo structure discussed previously. In accord with Wade's rules, reduction of this cluster to either $B_{10}H_{10}^{4-}$ or $B_{10}H_{10}^{6-}$ changes the shape of the cluster to the nido and arachno forms illustrated in Figure 4. The geometries of each of these species can be derived from X-ray studies, and therefore we can compare directly the energies of these three geometries.[19] We do so by the method described previously, in which we scale two of the clusters to have the same variance as that found in the third. We compare these energies as a function of the number of valence electrons. In Figure 10d we plot the difference in electronic energies between the nido $B_{10}H_{10}^{4-}$ cluster and each of the other two clusters. In this figure we adopt the following convention as to the sign of this difference of energies. We choose the sign so that, at any given electron count, the structure whose corresponding curve is the most positive (i.e., one closest to the top) is the stable structure. For the absissca we use the number of valence electrons per BH unit. Thus in $B_{10}H_{10}^{2-}$, $B_{10}H_{10}^{4-}$, and $B_{10}H_{10}^{6-}$ there are respectively 4.25, 4.50, and 4.75 electrons per BH unit (e/BH). According to our calculations, at these three electron counts the closo, nido, and arachno forms are respectively the most stable geometries. The results of our calculations therefore are in perfect agreement with the known experimental geometries. We have also considered in a similar manner the $B_6H_6^{n-}$, $B_8H_8^{n-}$, and $B_9H_9^{n-}$ families (n = 2, 4, 6) of clusters. In each of these cases, there is again a perfect match between experiment and theory. Furthermore, these are the only four cases where the closo, nido, and arachno geometries can be directly derived from X-ray structural work.[20] These results strongly indicate not only that we might be able to consider change in point group symmetry but also that our calculational method models correctly the forces responsible for Wade's rules.

Conclusions

In this paper we have shown that a properly modified Hückel theory can model well the bond length variations found in various homoatomic clusters and elemental structures. In one sense, this conclusion is not altogether surprising. It has been known for a long time that the Hückel bond order and overlap populations can successfully account for such bond length variations. From another viewpoint however, these results are surprising. It is generally believed that Hückel calculations are numerically far inferior to ab-initio Hartree–Fock calculations. However, we have shown almost uniformly across the periodic table that we can use Hückel theory to correctly model bond-breaking processes.[21] It is clear that the rather naive Hückel theory does indeed capture the nature of the chemical bond in the highly covalent systems discussed in this article.

Acknowledgment. We thank Ami Hatta and Cyndi Wells, who helped carry out the calculations on the gallium structure. This research was supported by the donors of the Petroleum Research Fund, administered by the American Chemical Society. Our research would not have been possible without the computer programs developed by R. Hoffmann, M.-H. Whangbo, M. Evain, T. Hughbanks, S. Wijeyesekera, M. Kertesz, C. N. Wilker, C. Zheng, J. K. Burdett, and G. Miller.

Appendix

We briefly review the underlying assumptions of the second-moment-scaling procedure. The goal of this method is to estimate in an effective way the total electronic energy, E_T. We first assume that $E_T = U(r) - V(r)$ where U is the hard-core atomic repulsion, V is the attractive bonding term, and r is a parameter which corresponds to the overall size of the system. We assume that Hückel theory correctly estimates the value of $V(r)$. We then follow the idea of Heine et al.[22] that the repulsion energy is

(19) We obtained atomic coordinates either directly from single-crystal X-ray structures of the desired borane or from application of Wade's rules to the known X-ray structure of the closo parent. We used boron positions from $B_{10}H_{10}^{2-}$, $B_{10}H_{14}$, and $B_{12}H_{12}^{2-}$ to produce respectively the closo, nido, and arachno 10-vertex polyhedra. In the last case we removed two of the original vertices so as to produce a $B_{10}H_{10}^{6-}$ cluster. The experimental values are taken from the following sources. (a) $B_{10}H_{10}^{2-}$: Reference 14c. (b) $B_{10}H_{14}$: Kasper, J. S.; Lucht, C. M.; Harker, D. *Acta Crystallogr.* **1950**, *3*, 436. (c) $B_{12}H_{12}^{2-}$: Wunderlich, J. A.; Lipscomb, W. N. *J. Am. Chem. Soc.* **1960**, *82*, 4427.

(20) Neither $B_7H_7^{2-}$ nor $B_{11}H_{11}^{2-}$ has been characterized by X-ray single-crystal studies. The structures of $B_6H_6^{2-}$, $B_8H_8^{2-}$, and $B_9H_9^{2-}$ have all been determined by single-crystal X-ray studies. The boron positions of $B_6H_6^{2-}$, $B_9H_9^{4-}$, and $B_9H_9^{6-}$ were taken to be the boron positions found in respectively B_6H_{10}, B_9H_{12}, and B_9H_{15}. The boron positions of $B_6H_6^{6-}$ and $B_8H_8^{6-}$ were both derived from the parent closo structures from which the appropriate vertices were removed. The experimental values were taken from the following sources. (a) $B_6H_6^{2-}$: Schaeffer, R.; Johnson, Q.; Smith, G. S. *Inorg. Chem.* **1965**, *4*, 917. (b) $B_8H_8^{2-}$ (also used to derive $B_6H_6^{6-}$): Reference 14a. (c) $B_9H_9^{2-}$ (also used to derive $B_8H_8^{4-}$): Reference 14b. (d) B_6H_{10}: Hirshfeld, E. L.; Eriks, K.; Dickerson, R. E.; Lippert, E. L.; Lipscomb, W. N. *J. Chem. Phys.* **1951**, *28*, 56. (e) $B_9H_{12}^-$: Jacobsen, G. B.; Meina, D. C.; Morris, J. H.; Thomson, C.; Andrews, S. J.; Reed, D.; Welch, A. J.; Gains, D. F. *J. Chem. Soc., Dalton Trans.* **1985**, 1645. (f) B_9H_{15}: Dickerson, R. E.; Wheatley, P. J.; Howell, P. A.; Lipscomb, W. N. *J. Chem. Phys.* **1957**, *27*, 200. (g) $B_8H_8^{6-}$ was derived from $B_{10}H_{10}^{2-}$: see ref 14c.

(21) It is well-known that the classical or restricted Hartree–Fock model is unable to model the energetics of bond breaking. This difficulty is generally called the dissociation problem. It is discussed in: Szabo, A.; Ostlund, N. S. *Modern Quantum Chemistry*; Macmillan: New York, 1982; p 221.

(22) Heine, V.; Robertson, I. J.; Payne, M. C. In *Bonding and Structure of Solids*; Haydock, R., Inglesfield, J. E., Pendry, J. B., Eds.; Royal Society: London, 1991.

proportional to the coordination numbers of the atoms in the system, C. This repulsion energy is due to "Coulomb repulsion of the nuclei and the exclusion principle in the overlap of the atoms".[22] As has been shown by Friedel and Cyrot-Lackmann[23]

$$C = \alpha\mu_2 \equiv \alpha\int_{-\infty}^{\infty} E^2\,\rho(E,r)\,dE$$

where $\rho(E,r)$ is the electronic density of states of the valence bands, which itself is (among other things) a function of the overall size of the system. We therefore find that the total energy E_T is

$$E_T = \alpha\int_{-\infty}^{\infty} E^2\,\rho(E,r)\,dE + \int_{-\infty}^{E_F} E\,\rho(E,r)\,dE$$

The first term on the right-hand side of the equation is the repulsive energy, $U(r)$, while the second term is the attractive energy, $-V(r)$. The term E_F refers to the Fermi energy for the system in question. We now follow the argument first discussed by Pettifor.[24] We consider two systems which we label 1 and 2. The terms E_{T1}, U_1, V_1, E_{T2}, U_2, and V_2 refer to the various energies of these two systems. We wish to perform calculations where $\Delta E = E_{T1} - E_{T2}$. It may be seen that

$$\Delta E = U_1(r_{1eq}) - V_1(r_{1eq}) - U_2(r_{2eq}) + V_2(r_{2eq})$$

where r_{1eq} and r_{2eq} refer to the respective equilibrium sizes of the two systems.

We use the fact that we are interested in equilibrium geometries in the following way. Note that near equilibrium E_{Ti} is constant. Therefore

$$U_2(r_{2eq}) - V_2(r_{2eq}) = U_2(r_{2eq}+d) - V_2(r_{2eq}+d)$$

In particular, we choose a value for d such that $U_2(r_{2eq}+d) = U_1(r_{1eq})$. We now find that

$$\Delta E = \int_{-\infty}^{E_{F1}} E\,\rho_1(E,r_{1eq})\,dE - \int_{-\infty}^{E_{F2}} E\,\rho_2(E,r_{2eq}+d)\,dE \quad (1)$$

We determine the value r_{1eq} from the true experimental size factor and $r_{2eq} + d$ from the equality

$$\int_{-\infty}^{\infty} E^2\,\rho_2(E,r_{2eq}+d)\,dE = \int_{-\infty}^{\infty} E^2\,\rho_1(E,r_{1eq})\,dE$$

This last expression is equivalent to stating

$$\mu_2(r_{2eq}+d) = \mu_2(r_{1eq}) \quad (2)$$

It may be seen that eqs 1 and 2 correspond exactly to the second-moment-scaling hypothesis.

(23) (a) Friedel, J. *Adv. Phys.* **1954**, *3*, 446. (b) Cyrot-Lackmann, F. *J. Physiol. (Paris), Suppl.* **1970**, *C1*, 67.
(24) Pettifor, D. G. *J. Phys. C: Solid State Phys.* **1986**, *19*, 285.

Empirical Force-Field Models for the Transition States of Intramolecular Diels–Alder Reactions Based upon ab Initio Transition Structures

Laura Raimondi,[†] Frank K. Brown,[‡] Javier Gonzalez,[†,§] and K. N. Houk*,[†]

Contribution from the Department of Chemistry and Biochemistry, University of California, Los Angeles, Los Angeles, California 90024, and the Department of Chemistry, University of Pittsburgh, Pittsburgh, Pennsylvania, 15260. *Received June 10, 1991. Revised Manuscript Received February 22, 1992*

Abstract: A quantitative model based upon Allinger's MM2 force field has been devised to calculate the diastereoselectivity of intramolecular Diels–Alder (IDA) reactions. The parameters for the modified MM2 force field were derived whenever possible from ab initio calculations on the intermolecular transition structures for the Diels–Alder reactions of butadiene plus ethylene, acrolein, and acrolein coordinated to BH_3. The force field reproduces the ab initio 3-21G transition structures for the intramolecular Diels–Alder reactions of 1,3,8-nonatriene and 1,3,9-decatriene. The force field was developed for both thermal and acid-catalyzed reactions and provides insight into the origins of the diastereoselectivity in the IDA cycloaddition for a wide variety of nonatrienes and decatrienes. The flexibility of the transition structure and the conformational effects due to the chain connecting the two reacting moieties were shown to be of the greatest importance in determining the stereochemical outcome of these reactions. The use of the parameters in the new MM3 force field was tested.

Introduction

The Diels–Alder cycloaddition is among the most powerful tools in organic synthesis,[1,2] since it allows a direct access to cyclic, highly functionalized systems in a regioselective and stereocontrolled way. The reaction conserves the stereochemistries of the diene and alkene,[1,2] and a stereocenter on one or both the reactants is often able to influence the relative stereochemistry of the newly formed stereogenic centers in the products.[2] Thus, both the relative and the absolute configuration at all the stereocenters can be controlled in the synthesis of highly functionalized molecules, provided that the factors influencing the diastereoselectivity are known and predictable.

Even greater control is possible when both reactants are part of the same molecule: intramolecularity enhances the factors

[†] University of California, Los Angeles.
[‡] University of Pittsburgh.
[§] On leave from the Department of Organometallic Chemistry, Universidad de Oviedo, 330011-Oviedo, Spain.

(1) Some reviews of the Diels–Alder reaction: (a) Martin, J. G.; Hill, R. K. *Chem. Rev.* **1961**, *61*, 537–562. (b) Sauer, J. *Angew. Chem., Int. Ed. Engl.* **1966**, *5*, 211–230. (c) Sauer, J. *Angew. Chem., Int. Ed. Engl.* **1967**, *6*, 16–33. (d) Houk, K. N. *Acc. Chem. Res.* **1975**, *8*, 361–369. (e) Sauer, J.; Sustmann, R. *Angew. Chem., Int. Ed. Engl.* **1980**, *19*, 779–807. (f) Gleiter, R.; Bohm, M. C. *Pure Appl. Chem.* **1983**, *55*, 237–244.
(2) Some reviews of asymmetric Diels–Alder reactions: (a) Paquette, L. A. In *Asymmetric Synthesis*; Morrison, J. D., Ed.; Academic Press: New York, 1984; Vol. 3, pp 455–501. (b) Oppolzer, W. *Angew. Chem., Int. Ed. Engl.* **1984**, *23*, 876–889. (c) Helmchen, G.; Karge, R.; Weetman, J. In *Modern Synthetic Methods*; Scheffold, R., Ed.; Springer Verlag: Berlin, 1986; Vol. 4, pp 261–306. (d) Oppolzer, W. *Angew. Chem., Int. Ed. Engl.* **1987**, *43*, 1969–2004.

0002-7863/92/1514-4796$03.00/0